

Syngas production by thermochemical conversion of CO₂ and H₂O using a high-temperature heat pipe based reactor

Howard Pearlman and Chien-Hua Chen

Advanced Cooling Technologies, Inc., 1046 New Holland Ave, Lancaster, PA, USA 17601

ABSTRACT

The design of a new high-temperature, solar-based reactor for thermochemical production of syngas using water and carbon dioxide will be discussed. The reactor incorporates the use of high-temperature heat pipe(s) that efficiently transfer the heat from a solar collector to a porous metal oxide material. Special attention is given to the thermal characteristics of the reactor, which are key factors affecting the overall system efficiency and amount of fuel produced. The thermochemical cycle that is considered is that for ceria based material. Preliminary data acquired from an early stage reactor, operated at temperatures up to 1100°C, is presented and efforts are now underway to increase the operating temperature of the reactor to 1300°C to further increase the efficiency of the thermochemical fuel production process.

Keywords: Thermochemical cycle, CO₂ utilization, Water splitting, Solar fuels

1. INTRODUCTION

Energy sustainability and climate change are two major challenges in the 21st century. One proposed renewable energy strategy to address both concerns involves the use of a thermochemical cycle to convert CO₂ and H₂O to CO and H₂ (syngas) using concentrated solar energy to drive the endothermic reduction portion of the cycle. The process works by cyclically changing the thermodynamic state of the working material to convert the thermal energy to chemical energy. While the process may involve multiple reaction steps, the overall reaction is water or CO₂ splitting (e.g., H₂O → H₂ + ½ O₂). The produced syngas can subsequently be converted into liquid fuels using the Fischer-Tropsch process or used to synthesize chemicals and other materials [1].

Early work on the thermochemical water splitting cycle aimed to use thermal energy from nuclear reactors, rather than from concentrated solar energy, to provide the necessary heat to drive the high temperature endothermic step in the process (~ 750-850°C). Those cycles often involved several steps and challenging separation processes. In particular, several hundred thermochemical cycles have been identified in the past 30-40 years and detailed screening of the cycles based on the number of reaction steps, operating temperatures, cycle efficiency, etc. has been studied [2]. More recently, relatively simple two-step cycles based on the alternate reduction and oxidation of metal oxides have received increased attention. For two-step cycles, the reduction temperature is generally higher (~1500°C), which can be provided by concentrated solar power (CSP). Several different metal oxides have been studied with a focus on iron oxide (Fe₃O₄/FeO) and zinc oxide (ZnO/Zn). However, the high temperature requirement introduces practical challenges regarding the stability of the metal oxides and the structural materials used for the reactor containment. As such, materials researchers have been actively screening candidate materials and trying to lower the reduction temperature while maintaining high fuel productivity/ efficiency and the simplicity of the cycle.

While most efforts in this area focus on the material development, research [3] shows that the overall solar-to-fuel efficiency of the process is highly dependent on the effectiveness of the heat transfer process, notably how the solar thermal energy is transferred to the material. In this work, a simple analysis of the heat transfer in the solar reactor is discussed. A heat pipe based reactor was proposed to enhance the heat transfer of the concentrated solar power into the metal oxide material. By leveraging the heat pipe working principle, it is also possible to perform the thermal cycle without moving parts.

1.1 Two-Step Thermochemical Cycle

The production of fuels from the thermochemical cycling of metal oxides occurs in two steps: (1) thermal reduction of the metal oxide at high temperatures, which generates oxygen; and (2) re-oxidation of the reduced metal oxide at lower temperatures by steam and/or carbon dioxide, which produces the chemical fuel (Fig. 1).

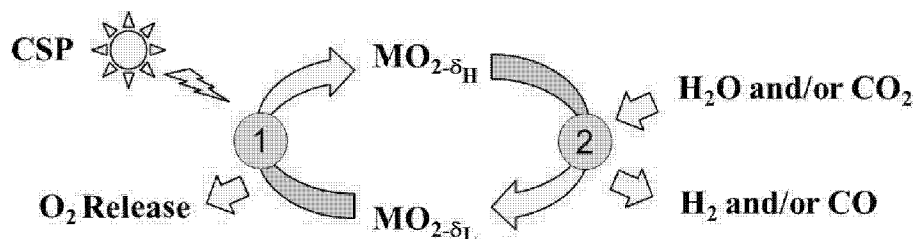
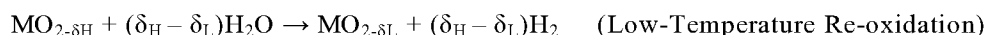


Figure 1. Two-step solar thermochemical cycle. Metal oxide (MO_2) is thermally reduced at high temperature (step 1) and re-oxidized by H_2O and/or CO_2 to produce H_2 and/or CO (step 2).

The thermochemical reactions for the production of hydrogen, specific to a metal oxide with variable oxygen content, can be written in the following form:



where MO represents a metal oxide, M is the metal of variable oxidation state (with dopant(s), if applicable), and δ_H and δ_L are the high and low temperature oxygen nonstoichiometry values relative to an ideal structure with stoichiometry MO_2 . The difference between δ_H and δ_L directly corresponds to the quantity of fuel produced in each cycle.

From the description given above, it is apparent that the thermal reduction step is, from an operational perspective, largely independent of the subsequent fuel generation step. Moreover, the oxygen release is critically dependent on the temperature and oxygen partial pressure. For typical metal oxides, temperatures in the range of 1400°C to 1600°C (in an inert gas environment, for example, having an oxygen partial pressure $P_{\text{O}_2} \sim 10^{-5}$ - 10^{-6} atm) are required to achieve nonstoichiometry changes on the order of 0.10 [4, 5].

Whether a particular reduced metal oxide is suitable for subsequent H_2O and/or CO_2 dissociation depends on both thermodynamic and kinetic factors. Specifically, the thermodynamics must be such that the reduced metal oxide has sufficient reducing power to drive the dissociation reaction. Furthermore, the oxygen must diffuse through the reduced metal oxide material at a sufficiently fast rate during the thermal reduction half-cycle and the kinetics must be sufficiently fast during the re-oxidation (dissociation) half cycle. Recently, ceria based materials have attracted attention. The ceria cycle is conceptually similar to that of other metal oxides, but differs in that the reduced and oxidized states do not correspond to distinct phases (in contrast to other cycles, e.g., the ferrite cycle $\text{FeO}/\text{Fe}_3\text{O}_4$). Accordingly, the extent of reduction or equivalently the stoichiometry change can be of arbitrary value. The advantages of ceria based materials are fast reduction and re-oxidation rates, good oxygen ion conduction, a high O_2 diffusion rate, no phase change at high temperature, and no carbon deposits formed during the low-temperature re-oxidation step.

In addition, it has been shown that the use of dopants can lower the temperature needed for thermal reduction (compared to the otherwise undoped material) and increase the conversion efficiencies [6]. Consequently, a zirconium (Zr) substituted ceria material (ZSC) with 18.5% (by mass) Zr was in this experimental work.

1.2 Thermal Issues Affecting Thermochemical Cycle Reactor Design

Unlike other water or CO_2 splitting methods, such as electrolysis or photoelectrochemical processes, the thermochemical cycle involves the conversion of thermal energy into chemical potential. As such, the attainable efficiency of the cycle is governed by the second law of thermodynamics and is affected by how efficiently heat is transferred into and out of the material. In addition, the cyclic nature of the process implies that the system is transient rather than steady-state. Figure 2A shows the thermal energy flow for a thermochemical cycle. After the thermal energy is collected and absorbed by the (solar) receiver, it is subsequently transferred to either the working material, the reactor structure (housing), or the environment by re-radiation from the heated surface; the distribution of thermal energy depends on the relative magnitude of their thermal resistances (Fig. 2B). Clearly, to maximize the system efficiency, most of the thermal energy needs to be used for heating the working material rather than be lost to the environment or used to heat the reactor structure. Therefore, the goal of our thermal design is to minimize the thermal resistance of the metal oxide material.

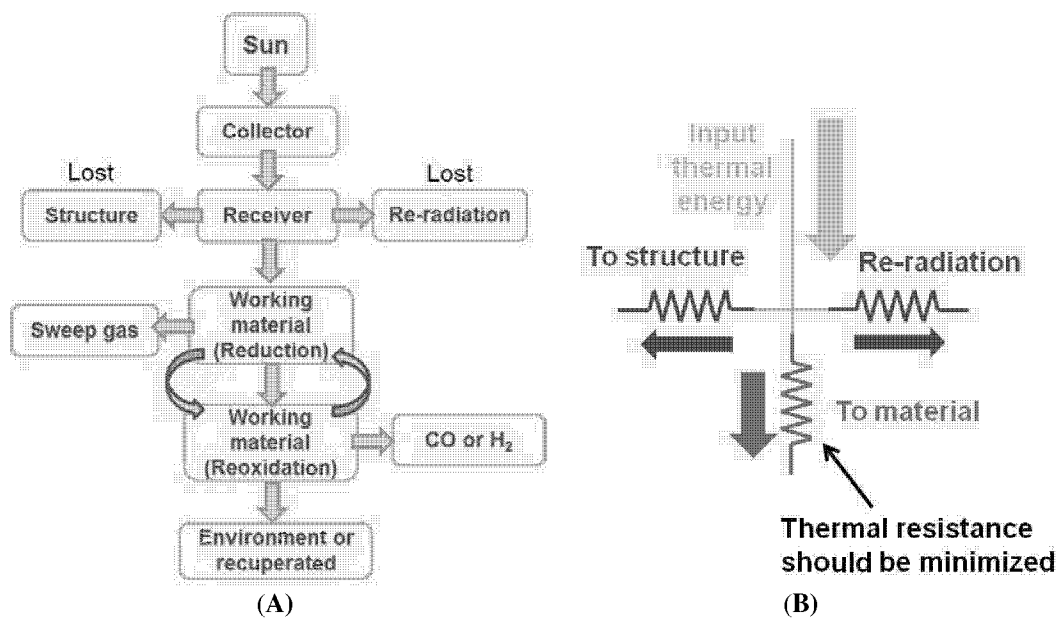


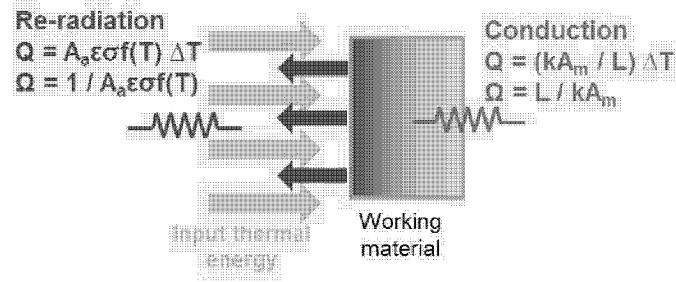
Figure 2. (A) Thermal energy flow analysis for a thermochemical cycle. The heat absorbed by the solar receiver is either used to heat the structural material, re-radiated to the environment, or transferred to the metal oxide material. The thermal resistance between receiver and working material should be minimized to maximize the heat transfer into the material and thus maximize the solar to fuel efficiency. (B) Sketch showing the relevant thermal resistances. Note that the portion of overall thermal energy transferred to the material is determined by the relative magnitude of the thermal resistances.

For a fixed bed type reactor design [7], the dominant thermal resistance is the conduction resistance into the material (Fig. 3A) since the porous ceria-based material has a very low thermal conductivity. For example, the effective thermal conductivity (k) of porous ceria with 80% porosity is less than $0.1\text{W/m}\cdot\text{K}$ (Ar sweep gas). The high thermal resistance of the material results in the surface of the material being heated very rapidly, as a steep temperature gradient is formed through the material. At high temperature, the re-radiation resistance is also relatively low such that most of the thermal energy re-radiates back to the environment rather than conducting into the material to thermally reduce it. To lower the conduction resistance, the material thickness (L) can be decreased and/or the heat transfer area (A_m) increased. At the same time, there is an additional requirement on the amount of material needed to convert a given amount of H_2O or CO_2 to H_2 or CO and achieve the theoretical efficiency; as such, the amount of material cannot simply be decreased to reduce the thickness of the material layer and thus decrease the conduction resistance. Rather, the material must be distributed in a thin layer and the heat transfer area should be increased such that the given amount of material can be rapidly heated/ thermally reduced. A heat pipe based reactor allows the heat transfer area to be increased and is therefore proposed to achieve this goal; this is discussed in Section 1.3.

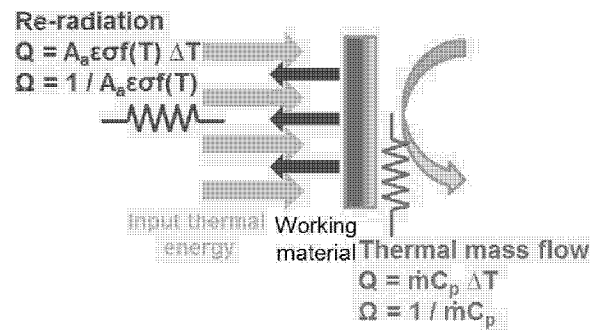
For a moving bed type reactor design [8, 9] (rather than a packed bed), a similar thermal analysis must be done. In such a configuration, a thin layer of material is typically placed on a large rotating wheel. In this case, the dominant thermal resistance depends on the thermal mass flow rate (Fig. 3B), which in turn depends on the rotation speed of the wheel. While the conduction resistance may not be large for a reactor with a thin metal oxide layer, other factors including the chemical time for re-oxidation may limit the allowable rotation rate and thus affect the system level efficiency. For example, the rotation speed may not be limited by the reduction thermal time scale, but rather by the re-oxidation chemical time scale, which depends on the kinetics. Clearly, to maximize the system level efficiency, both thermal and chemical time scales for the thermal reduction and re-oxidation steps would ideally be balanced such that the moving bed can operate at a fixed rotation speed.

The effect of increasing heat transfer area can be further explained by the following example. For a material with thickness 1 cm and 80% porosity, if the heat transfer area (A_m) is 10 times that of the aperture area A_a and the material surface temperature is 1000K, the thermal resistance for re-radiation to the environment is equal to the conduction resistance through the material (Fig. 3C). This means that 50% of the input thermal energy will re-radiate back to the

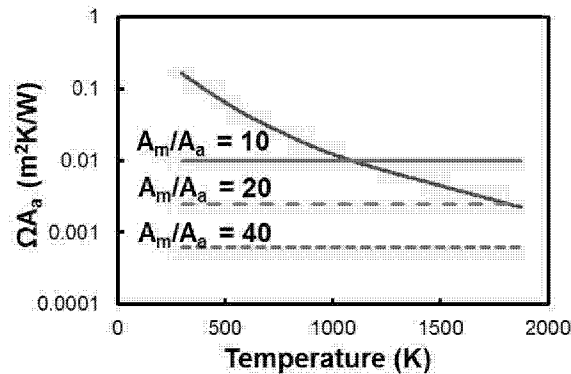
environment. By increasing the A_m/A_a ratio, the conduction thermal resistance can be decreased so that more input thermal energy will be transferred into the working material than re-radiated back to the environment.



(A)



(B)



(C)

Figure 3. Schematic showing the dominant thermal resistances (re-radiation vs. conduction through the working material) for a: (A) Fixed bed type reactor and (B) a Moving bed reactor. Here, A_a is the receiver aperture area and the strength of re-radiation is the function of the material surface temperature. In conduction heat transfer, A_m is the heat transfer area to the material, k is the material thermal conductivity, and L is the material thickness. Assuming conduction to the working material is not the dominant thermal resistance, the thermal resistance associated with the thermal mass flow (dependent on the wheel rotation speed) will dominate. (C) Thermal resistances for re-radiation (red line) and conduction (green lines) vs. temperature.

1.3 Heat Pipe Based Reactor Design

A new heat pipe based solar reactor was designed and a prototype demonstrating the overall principle was developed in this work. The focus was to increase the heat transfer area to enable rapid heating of the ceria-based material subject to a

concentrated solar heat flux. In this design, the incident solar flux is directed into a cavity receiver containing one or more high-temperature heat pipes. Specifically, the evaporator of the heat pipe is connected to the cavity housing where the incident solar flux is then transferred to the material via the heat pipe. The condenser end of the heat pipe is located outside of the cavity. The length of the condenser can be tailored to effectively spread the concentrated solar radiation over a large surface area. The porous ceria material would then be located around the condenser end of the heat pipe. A key attribute of this design is that it enables the ceria material to be distributed over a large surface area (determined by the condenser length and number of heat pipes) and provides a high degree of flexibility to optimize the heat transfer from the concentrated solar power to the ceria material. Another advantage of a heat pipe based reactor is to perform thermal cycling without moving parts. Specifically, a combination of pressure controlled heat pipe (PCHP) and constant conductance heat pipe developed by ACT [10] enables the thermal load to be varied by adjusting the amount of the non-condensable gas at the condenser end of the PCHP (Fig. 4). In effect, controlling the amount of non-condensable gas controls the available heat transfer area at the condenser, which in turn enables thermal regulation of the CSP to the ceria material.

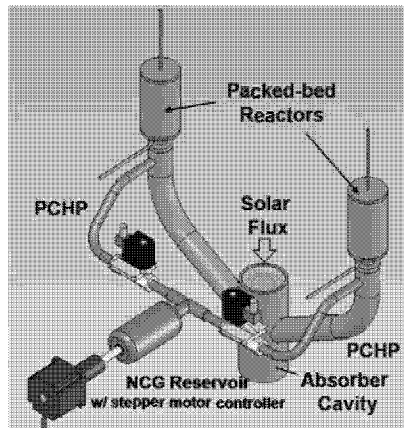


Figure 4. Preliminary concept for a dual heat pipe based packed bed reactor. Two reactors are cyclically heated by the concentrated solar energy. Pressure controlled heat pipes (PCHP), controlled by the amount of non-condensable gas (NCG), are used to perform the thermal cycle and two constant conductance heat pipes (CCHP) are used to isothermize and transfer the thermal energy to the packed bed reactors.

A heat pipe can be thought of as a *thermal transformer* that converts the high heat flux, concentrated solar energy at the solar receiver to a lower heat flux that is applied to heat the ceria material. In addition, the heat pipe reactor enables the material to be distributed over a large surface area (having a large surface area to volume ratio), which accelerates the transient thermal response of the material, shortens the reduction half-cycle time, and in turn increases the system efficiency. Also, since the heat pipe reactor decouples the heat transfer area of the material (condenser surface area of the heat pipe) from the heat transfer area of the cavity receiver (evaporator area of the heat pipe), the solar receiver can be relatively small such that the overall heat loss (e.g., re-radiation through the aperture) can be minimized.

The thermochemical cycle can perhaps also be thought of in an analogous way to a thermodynamic cycle, in which mechanical work results from the net difference between the thermal energy into and out from the working fluid. In the thermochemical cycle, the chemical energy (enthalpy of combustion of H₂ or CO) obtained is equal to the net thermal energy difference applied to the “working material” (ceria). A dish stirling engine provides a good example to further demonstrate how important heat transfer is in such systems. If the working fluid is helium, which has the second highest thermal conductivity among the gases (behind hydrogen), a cavity receiver can handle a heat flux capability (~75 W/cm²) at elevated helium pressures. If the working fluid is changed to air, which has a much lower thermal conductivity, the output power will be only 20-25% for the same displacement engine design [11], which is 4-5 times lower efficiency for the same input thermal power. For the thermochemical cycle, since the thermal conductivity of the working material is for the most part fixed (dependent on material, porosity, etc.), increasing heat transfer area is necessary for the high heat flux produced inside the solar receiver to be transferred to the material rather than re-radiated back to the environment in an effort to maximize the efficiency and approach the theoretical limit.

2. EXPERIMENTAL SETUP

To assess the feasibility of a heat pipe based reactor, a single heat pipe reactor system was designed and tested. An overall schematic of the system is shown in Fig. 5. The packed bed reactor contains a porous sintered zirconia-ceria material. The material was synthesized from commercially-available, micron-size cerium oxide (CeO_2) and zirconium oxide (ZrO_2) powders that were ball milled and sintered at 1500°C for 24 hours. The packed bed was formed in an annular configuration and positioned concentrically around a high-temperature heat pipe that both transferred heat into the reactor and aided in isothermalizing the packed bed. Haynes 230 was chosen as the heat pipe envelope based on its excellent creep strength, oxidation resistance, ability to machine, and ability to operate continuously at temperatures up to 1100°C . The internal working fluid in the heat pipe was sodium, which is effective for temperatures up to 1100°C .

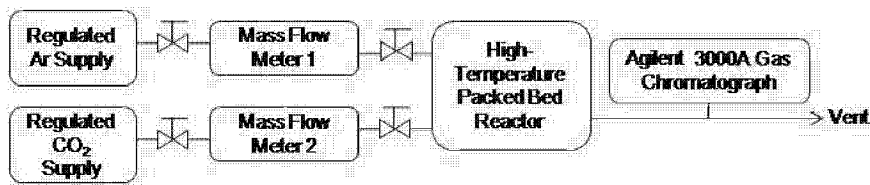


Figure 5: Overview of the experimental thermochemical reactor system.

An image of high-temperature reactor is shown in Fig. 6A along with photos of the actual hardware (Fig. 6B) and reactor housing (Fig. 6C). At the base of the reactor, a SiC spiral heater element (I Squared R Element Co.) was positioned concentrically around the evaporator-end (bottom) of a vertically oriented constant conductance heat pipe (1" diameter and 12" long). The resistive heater element simulated the incident concentrated solar flux that can be generated from a solar collector. The heat was transferred upwards into the reactor volume, which contained the packed bed material (67 g) in the annulus (4.45 mm wide) between the outer wall of the heat pipe and the inner wall of the reactor housing; it was concentrically located around the condenser-end (top) of the heat pipe. The heat pipe also aided in isothermalizing the packed bed (Fig. 7). Figure 8 shows the initial testing of the heat pipe prior to integration with the reactor assembly.

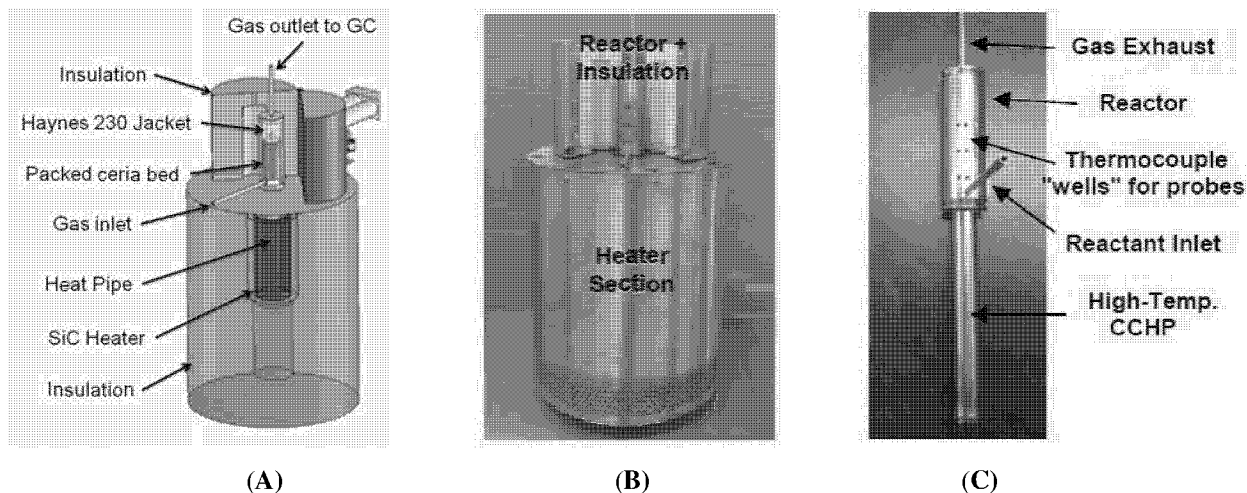


Figure 6. Experimental heat pipe based reactor. (A) Schematic of the experimental setup containing a silicon carbide heating element (can be heated to 1650°C); (B) Actual test section, insulation and reactor housing; (C) Heat pipe and reactor.

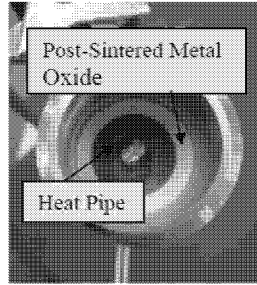


Figure 7. The packed bed surrounds the heat pipe obtaining high heat transfer area.

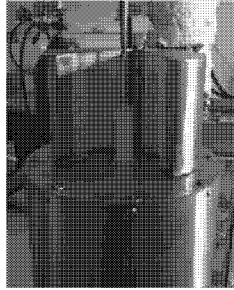


Figure 8. Initial testing of the heat pipe at high-temperature (1050°C) showing relative isothermality (uniform red color) prior to integration with the reactor assembly.

The experimental reactor was thermally cycled and the axial and the radial temperature distributions in the packed bed were recorded. A PID controller was used to regulate the power to the SiC heater based on feedback from a thermocouple in contact with the base of the heat pipe (T_{base}). Three temperature measurements ($T_{1,\text{inner}}$, $T_{2,\text{inner}}$, $T_{3,\text{inner}}$) are taken at 3 different axial locations along the condenser section of the heat pipe (in the reactor section, coinciding with the I.D. of packed bed) and three measurements ($T_{1,\text{outer}}$, $T_{2,\text{outer}}$, $T_{3,\text{outer}}$) taken at the outer radius of the packed bed at the same axial locations as the inner temperature measurements. All thermocouples were Omega Clad XL 0.0625" sheathed Type K. Here it should be noted that the thermocouples were inserted in "thermal wells" made from 0.25" O.D., 0.080" wall thickness Haynes 230 tubing that was welded closed at their interior ends and welded circumferentially to the outer reactor housing. These welds prevented air leaks from the reactor that could adversely affect the fuel productivity. Additionally, the temperature measurements across the packed bed ($T_{i,\text{outer}} - T_{i,\text{inner}}$) provided information on the radial temperature gradient across the packed bed. This is important since the relatively low thermal conductivity of the porous metal oxide limits the rate at which heat transferred from the heat pipe propagates radially into the ceria material. In turn, the temperature nonuniformity in the reactor affects the overall extent that the material can be reduced during the thermal reduction half-cycle (i.e., nonstoichiometry of the material). A spatial variation in the nonstoichiometry of the material will then affect the amount of fuel produced within the reactor during the re-oxidation half-cycle, i.e., reduce the amount of fuel produced relative to that which could otherwise be produced if the material was uniformly reduced at the higher temperature (inner temperature of the metal oxide).

During the high-temperature thermal reduction half-cycle, a "low oxygen content" Argon sweep gas (Praxair, Research Grade 6.0, 99.9999% purity) continuously flowed through the reactor at a prescribed flow rate. Oxygen gas released from the metal oxide was swept downstream and measured using an Agilent 3000A micro-gas chromatograph (GC) equipped with PoraPlotU and MolSieve 5A columns. During the lower temperature re-oxidation half-cycle, the inert sweep gas was turned off and CO_2 and/or H_2O vapor were introduced into the reactor (in some cases, CO_2 and H_2O were premixed with the sweep gas) at a prescribed mass flow rate. The effluent from the reactor was analyzed approximately every 3 minutes with the GC and the composition (i.e., H_2 , CO , CO_2 , etc.) determined.

3. RESULTS

3.1 Thermal Behavior of the Heat Pipe Reactor

The inner and outer temperature measurements of three different locations of the reactor are shown in Fig. 9. The axial temperature difference along the reactor ($T_{3, \text{inner}} - T_{1, \text{inner}}$) was about 40°C for ~ 5 cm distance. A representative plot of the average temperature difference across the packed bed is shown in Fig. 10 based on the average of the temperature measurements taken at the three axial locations. As shown, the temperature difference across the packed bed asymptotes to $\sim 20^\circ\text{C}$ at about $\sim 1/3$ of the thermal reduction half-cycle and about 10°C during the re-oxidation half-cycle.

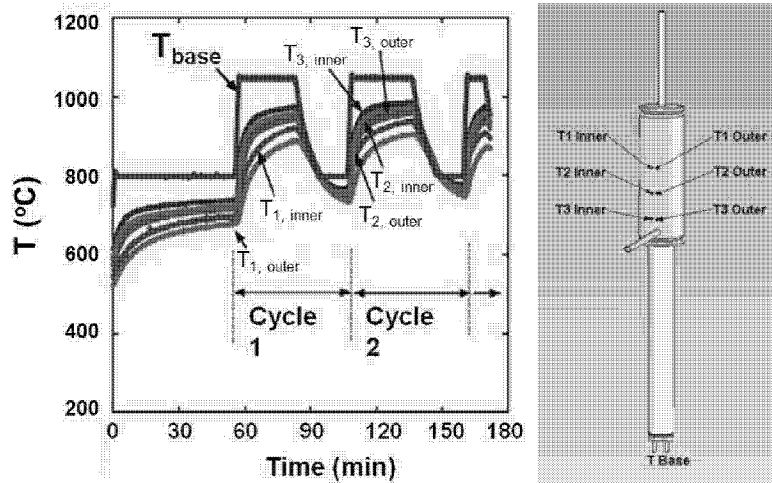


Figure 9. Temperature histories associated with thermal cycling of the zirconia-ceria material in the reactor; 1 SLPM Ar sweep gas. Right: the axial locations of the thermocouples measured from the base of the reactor housing upwards were: 2.22 cm, 4.76 cm, and 7.30 cm for T3, T2, and T1, respectively. "Inner" refers to the temperatures measured in the thermal wells closest to the heat pipe wall and "outer" refers to the outer radii of the packed bed nearest the internal wall of the reactor housing.

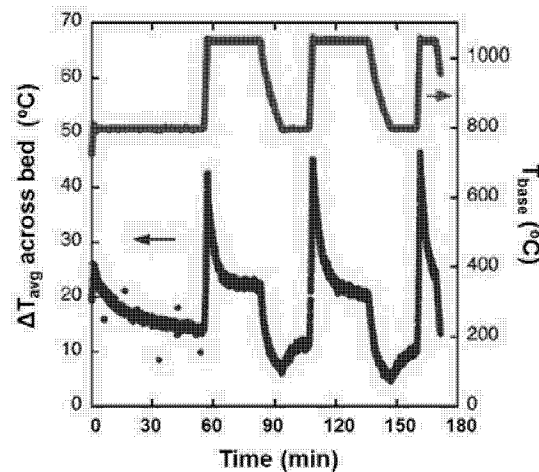


Figure 10. Average temperature difference across the packed bed as the function of time (1 SLPM Ar flow).

3.2 O_2 Evolution and CO_2 Dissociation

The dissociation of water and carbon dioxide are similar; as such, for convenience, dissociation of CO_2 was considered here. Figure 11 shows the oxygen and CO evolution rates in the reactor. The O_2 and CO concentrations (percentages by volume) of the downstream products were determined by gas chromatography and their evolution rates were then

computed knowing the Ar and CO₂ flow rates. While the overall fuel productivity was relatively low as compared with other reported results [3] (for which thermal reduction was at 1500°C as opposed to the 1000-1100°C temperatures used in this study), one interesting result was that the time for oxygen release was relatively short (80% of the O₂ produced in ~ 32 min). It is believed that the large heat transfer area contributed to the relatively small temperature gradient across the material (as shown in Fig.10) and overall short time required for the oxygen release. Another note is that the CO generation rate was comparatively slow (80% of CO produced in ~47 min.), perhaps not unexpectedly because the doped zirconium slows the kinetics of the re-oxidation reaction.

At this stage in the design, additional testing is being performed and a higher temperature reactor is also being designed using refractory metals. Modeling work is also being performed to predict the transient thermal performance of the reactor(s) including radiation transfer and simplified kinetics.

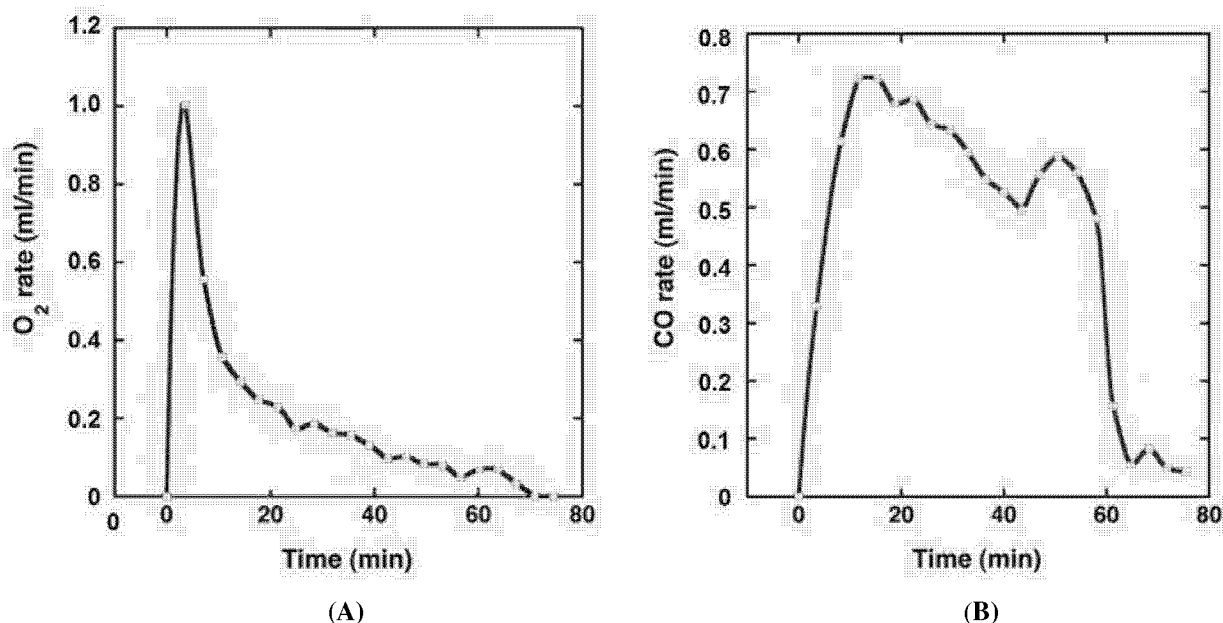


Figure 11. (A) O₂ evolution rate during thermal reduction reaction. Q_{Ar} = 1 SLPM. (B) CO evolution rate during re-oxidation reaction. Q_{CO2} = 4 SLPM.

4. CONCLUSION

A simple multi-dimensional thermal resistance model was used to explain the low system efficiency of current solar thermochemical reactors, which are now at ~2% or less. A heat pipe based thermochemical reactor was also developed with the focus on increasing the heat transfer area and reduce thereby reduce the thermal resistance to the working material. The thermal performance and O₂ release and CO production rates were demonstrated using CO₂ as the feedstock for select test conditions.

The current reactor is limited to operation at 1100°C due to creep stress of the nickel-based alloy material (Haynes 230). To further increase fuel productivity, the reactor temperature needs to be further increased (to 1300-1500°C) and additional work aimed at lowering the reduction temperature of metal oxides without adversely affecting their re-oxidation kinetics is also needed.

For higher temperature operation, a refractory metal heat pipe reactor encapsulated in a quartz vacuum tube (to suppress oxidation) is now under development by the authors. In this new reactor design, heat is transferred solely by radiation from the heat pipe to the working material. As discussed, the reactor design focuses on reducing the thermal resistance and the timescale needed to uniformly heat the packed bed. To accomplish this, the new reactor will have a large heat transfer surface area required for the incident solar energy to rapidly be transferred to the working material such that it can be uniformly reduced while minimizing re-radiation loss. As noted, the heat pipes in these designs simply act as a

fin structure with nearly perfect fin efficiency to efficiently distribute the concentrated solar power to the metal oxide material in the reactor.

ACKNOWLEDGEMENTS

The authors wish to express their sincerest thanks to Dr. Rich Diver, Dr. Yong Hao, and Professor Sossina Haile for useful discussions on the reactor design and materials selection. In addition, the authors wish to thank the Project Manager, Mr. Douglas Archer, and the DOE Office of Fossil Energy for financial support for this work under contract #DE-SC0004729.

REFERENCES

- [1] Song, C., "Global challenges and strategies for control, conversion and utilization of CO₂ for sustainable development involving energy, catalysis, adsorption and chemical processing," *Catalysis Today* 115, 2–32 (2006).
- [2] Abanades, S., Charvin, P., Flamant, G., Neveu, P., "Screening of water-splitting thermochemical cycles potentially attractive for hydrogen production by concentrated solar energy," *Energy* 31, 2805-2822 (2006).
- [3] Chueh, W., Falter, C., Abbott, M., Scipio, D., Furlur, P., Haile, S., Steinfeld, A., "High-Flux Solar-Driven Thermochemical Dissociation of CO₂ and H₂O Using Nonstoichiometric Ceria," *Science* 330, 1797-1801 (2010).
- [4] Panlener, R. J., Blumenthal, R. N. & Garnier, J. E., "A Thermodynamic Study of Nonstoichiometric Cerium Dioxide," *J. Phys. Chem. Solids* 36, 1213-1222 (1975).
- [5] Chueh, W.; Haile, S., "A thermochemical study of ceria: Exploring an old material for new modes of energy conversion and CO₂ mitigation," *Philosophical Transactions of the Royal Society* 368, 3269–3294 (2010).
- [6] Hao, Y., Chueh, W., and Haile, S., "Thermochemical Water Splitting with Zirconium-Substituted Cerium Oxides," Pacific Rim Meeting, Honolulu, Oct 7-12 (2012).
- [7] Furler, P., Scheffe, J., and Aldo Steinfeld, A., "Syngas production by simultaneous splitting of H₂O and CO₂ via ceria redox reactions in a high-temperature solar reactor," *Energy Environ. Sci.* 5, 6098-6103 (2012).
- [8] Diver, R., Siegel, N., Moss, T., Miller, J., Evans, L., Hogan, R., Allendorf, M., Stuecker, J., James, D., "Innovative Solar Thermochemical Water Splitting," Sandia Report SAND2008-0878 (2008).
- [9] Kaneko, H., Miura, T., Fuse, A., Ishihara, H., Taku, S., Fukuzumi, H., Naganuma, Y., and Tamaura, Y., "Rotary-Type Solar Reactor for Solar Hydrogen Production with Two-step Water Splitting Process," *Energy Fuels* 21 (4), 2287–2293 (2007).
- [10] Walker, K., Hartenstine, J., Tarau, C., Sarraf, D., and Anderson, W., "Low-Temperature, Dual Pressure Controlled Heat Pipes for Oxygen Production from Lunar Regolith," 15th IHPC, Clemson, USA (2010).
- [11] Martini, W. R., "Stirling Engine Design Manual," NASA CR-135382 Final Report (1978).
- [12] Mogensen, M., Sammes, N., Tompsett, G., "Physical, chemical and electrochemical properties of pure and doped ceria," *Solid State Ionics* 129, 63–94 (2000).
- [13] Miller, J., Allendorf, M., Ambrosini, A., Chen, K., Coker, E., Dedrick, D., Diver, R., Hogan, R., Ermanoski, I., Johnson, T., Kellogg, G., McDaniel, A., Siegel, N., Staiger, C., Stechel, E., "Reimagining Liquid Transportation Fuels: Sunshine to Petrol," Sandia Report Final Report (2012).